Optical spectroscopy of a single $Al_{0.36}In_{0.64}As/Al_{0.33}Ga_{0.67}As$ quantum dot

K. Hinzer, P. Hawrylak, M. Korkusinski, and S. Fafard
Institute for Microstructural Sciences, National Research Council, Ottawa, Ontario, Canada, K1A 0R6
and Physics Department, University of Ottawa, Ottawa, Ontario, Canada, K1A 6N5

M. Bayer,[1] O. Stern,[1] A. Gorbunov,[2] and A. Forchel[1]
[1]*Technische Physik, Universität Würzburg, Am Hubland, D-97074 Würzburg, Germany*
[2]*Institute of Solid State Physics, Russian Academy of Sciences, 142432 Chernogolovka, Russia*
(Received 31 August 2000; revised manuscript received 7 November 2000; published 31 January 2001)

We report results of interband spectroscopy of a single $Al_{0.36}In_{0.64}As/Al_{0.33}Ga_{0.67}As$ self-assembled quantum dot. The single dot spectroscopy has been carried out at low temperature as a function of the excitation power and magnetic field up to 8 T. The emission spectra as a function of excitation power show two distinct groups of transitions that we associate with the recombination from ground and excited quantum dot levels with a spacing of ~70 meV. The application of magnetic field allows us to identify the exciton emission as well as the emission from the biexciton, and charged exciton complexes with binding energies of ~5 meV. The binding energies compare favorably with results of calculations.

DOI: 10.1103/PhysRevB.63.075314 PACS number(s): 78.66.Fd, 78.55.Cr, 71.35.Gg, 71.70.Ej

Semiconductor self-assembled quantum dot (QD) heterostructures make excellent systems for basic physics studies,[1] as well as technological applications,[2,3] such as the QD lasers and detectors due to their high optical quality and the tunability of their energy levels. Most studies so far concentrated on material systems such as InAs/GaAs and $InGa_xAs_{x-1}$/GaAs with emission in the infrared.[4] For applications requiring visible emission, shorter wavelength systems such as the red-emitting $Al_xIn_{1-x}As/Al_yGa_{1-y}As$ quantum dots (QDs) are desired.[5] In InAs/GaAs based QDs, the quantized electron and hole energy levels of individual dots are clearly visible in the emission spectra from large ensembles as a function of the excitation power, and hence, increasing the population of carriers.[6] However, a much larger inhomogeneous broadening of the emission spectra of ternary $Al_xIn_{1-x}As$ imbedded in $Al_yGa_{1-y}As$ has prevented the demonstration of quantized zero-dimensional (0D) energy levels in these QDs. Indeed QD ensembles with visible 0D density of states can now be obtained from the $In_xGa_{1-x}As$/GaAs material system,[6–13] but $Al_xIn_{1-x}As/Al_yGa_{1-y}As$ QD ensembles with well-defined 0D electronic levels have not yet been achieved.[14–17] Nevertheless, techniques have been developed to permit the study of individual QDs, and therefore, to eliminate the inhomogeneous broadening problem.[14,16,18–28] Previous spectroscopic studies of small ensembles of $Al_xIn_{1-x}As/Al_yGa_{1-y}As$ QDs have shown properties characteristic of zero-dimensional systems such as extremely sharp homogeneous linewidths,[14,18] as well as invariant linewidths and lifetimes up to the onset of thermionic emission,[16] although no detailed study of the electronic properties of this system has yet been made.

In this paper, we use single dot spectroscopy to demonstrate the existence of quantized electron and hole energy levels in $Al_{0.36}In_{0.64}As$ QDs. The excited states and level spacing is obtained by measuring recombination from up to six exciton complexes. Extrapolating our results to higher excitation powers indicates approximately five confined electronic shells. In the intermediate pumping intensity regime, we present a magneto-optical study of an exciton, biexciton, and charged exciton complexes. These studies yield a large exciton g factor of ~2, biexciton binding energy of ~5 meV, and charged exciton energy very close to the biexciton energy. The measured emission spectra agree well with calculated emission spectra from exact diagonalization studies of exciton, charged exciton, and biexciton complexes.

I. QD ENSEMBLE PHOTOLUMINESCENCE

The layers are grown in a modified V80H molecular-beam epitaxy system using As_2.[29] The self-assembled QDs were obtained using the spontaneous island formation in the initial stages of the Stranski-Krastanow growth mode during the epitaxy of highly strained $Al_{0.36}In_{0.64}As$ on $Al_{0.33}Ga_{0.67}As$ layers, grown on (100) GaAs substrates. A 100-nm GaAs cap terminates the heterostructure. Transmission electron microscopy of similar samples indicate low dot densities, i.e., ~10–100 QDs/μm^2, and lens-shaped QDs having base diameters of ~20 nm and heights of ~5 nm.[15,17] Figure 1 shows the evolution of the low-temperature photoluminescence spectrum with increasing excitation intensity of a large number of QDs (>100 000). The excitation has been carried out with an Ar^+ laser above the $Al_{0.33}Ga_{0.67}As$ barrier. At the lowest excitation intensity, a peak centered at ~1.68 eV (738 nm) with an inhomogeneous linewidth of ~100 meV is observed. As the excitation power is increased, the emission peak becomes asymmetric and widens toward higher energies.[5] At these higher intensities, the peak from wetting layer (WL) emission is observed at 1.89 eV (655 nm). The presence of a WL signal in this system confirms a low QD density. The WL peak is located at the same energy as for control samples containing only a WL and no QDs (not shown). A third peak also is seen at 1.99 eV (622 nm). This peak corresponds to the emission from the barrier material, i.e., bulk $Al_{0.33}Ga_{0.67}As$. As the photoluminescence shows,

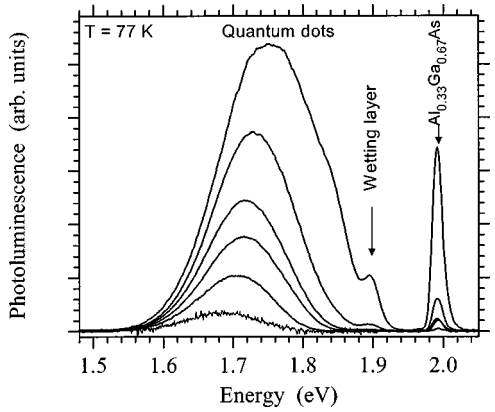

FIG. 1. Photoluminescence spectra of an ensemble of $Al_xIn_{x-1}As$ self-assembled QDs for excitation powers ranging from 0.15 W/cm^2 (bottom curve) to 2500 W/cm^2 (top curve).

in this ternary/ternary system, the emission originating from the different QD shells remains unresolved when probing a large amount of QDs.

II. SINGLE QD PHOTOLUMINESCENCE

To isolate a single QD, small fields were fabricated by electron-beam lithography and wet chemical etching on an unpatterned sample. The lateral sizes of the fields ranged from 2 μm down to 100 nm. The smallest fields contain a few, one or no QDs, and were optically probed with the 488 nm line of a cw Ar^+ laser with a spot size focused to a diameter of $\sim$20 μm. To reduce sample heating under optical excitation, the structures were held in superfluid helium at about 1.2 K in an optical cryostat. The sample emission was dispersed by a double monochromator ($f=0.6$ m) and detected with a LN_2-cooled Si charge-coupled-devices camera for 60 s accumulation times. For magneto-optical measurements, the magnetic field was aligned in the growth direction. The polarization of the luminescence was analyzed using a quarter-wave retarder and a linear polarizer.

Figure 2 displays the effects of reducing the number of QDs probed.[14] As the probe area is reduced, the inhomogeneous broadening vanishes and leaves way to sharp emission lines originating from individual QDs. When probing small enough mesas, spectra from a single QD can be observed. In the case shown, the chosen QD emits in the lower energy range of the QD ensemble. A linewidth of $\sim$1.0 meV is measured for these QDs. Two possible factors can explain this line broadening, first the processing used for etching down material to isolate a single QD introduces surface defects on the walls of the pillar containing the QD. These defects can get charged and discharged as a function of time (of the order of a nanosecond) and may lead to small variations in the QD confinement potential. When performing a measurement that lasts for seconds, these variations in confinement get averaged out increasing the homogeneous linewidth of $\sim$0.1 meV (Ref. 16) to $\sim$1 meV. As well, above barrier excitation can lead to linewidth broadening due to the presence of a large phonon population in the sample.

In Fig. 3(a), we present emission from an individual QD

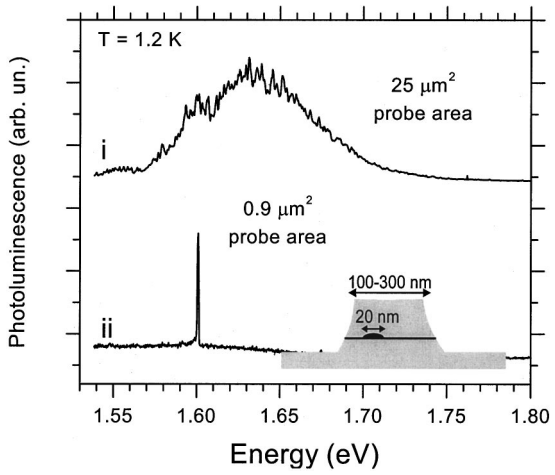

FIG. 2. Low excitation photoluminescence showing emission from the $Al_xIn_{x-1}As$ QDs when probing (i) an ensemble of $\sim$100 QDs in a large field and, (ii) a single QD in a small field. The schematic drawing shows a sample that has been etched to obtain a small field containing only one QD above the WL (dark area).

as a function of excitation power. At low excitation powers, only one sharp line is visible at 1.6008 eV. This is attributed to the recombination of a single electron-hole pair. As the excitation power is increased above 6 W/cm^2, a second peak appears at 1.5952 eV below the exciton line. At a pump power of 20 W/cm^2, two closely spaced peaks are observed at much higher energy, one at 1.6691 eV and the other at 1.6750 eV. In addition, many mostly unresolved peaks are observed over a range of $\sim$20 meV located just below the first two dominating peaks around 1.60 eV.

In order to explain the spectra further, we must look at a model for confined energy levels of QDs.[1,30–32] The bound states of both electrons and valence-band holes of a lens-shaped QD can be represented using an effective parabolic potential. The electronic energies $E^e_{mn}=\Omega^e_+(n+1/2)+\Omega^e_-(m+1/2)$, eigenstates $|mn\rangle$, and angular momenta $L^e_{mn}=m-n$ are those of two harmonic oscillators tunable with magnetic field B applied normal to the plane of the QD. Due to strain in the structure, the valence-band hole is treated in the effective-mass approximation as a positively charged particle with angular momentum $L^h_{mn}=n-m$, opposite to the electron, and energies $E^h_{mn}=\Omega^h_+(n+1/2)+\Omega^h_-(m+1/2)$. An example of the single-particle configuration of a two-shell QD is shown in Fig. 3(b). These QD shells are populated with an increasing number of carriers according to the Pauli exclusion principle. The s shell is twofold spin degenerate and cannot be occupied by more than two electron-hole pairs, the p shell is doubly degenerate and can hold a maximum of four electron-hole pairs. At very low excitation intensity, the QD is either empty or only one electron-hole pair is present in the s shell. The resulting emission line (X) clearly originates from a single exciton decay in the s shell. As the pump power increases, a second peak appears 5.0 meV below the exciton peak, and increases superlinearly with excitation power. This line is immersed in a growing background. We assign this line to the radiative recombination of a bound biexciton ($2X$) into a single exci-

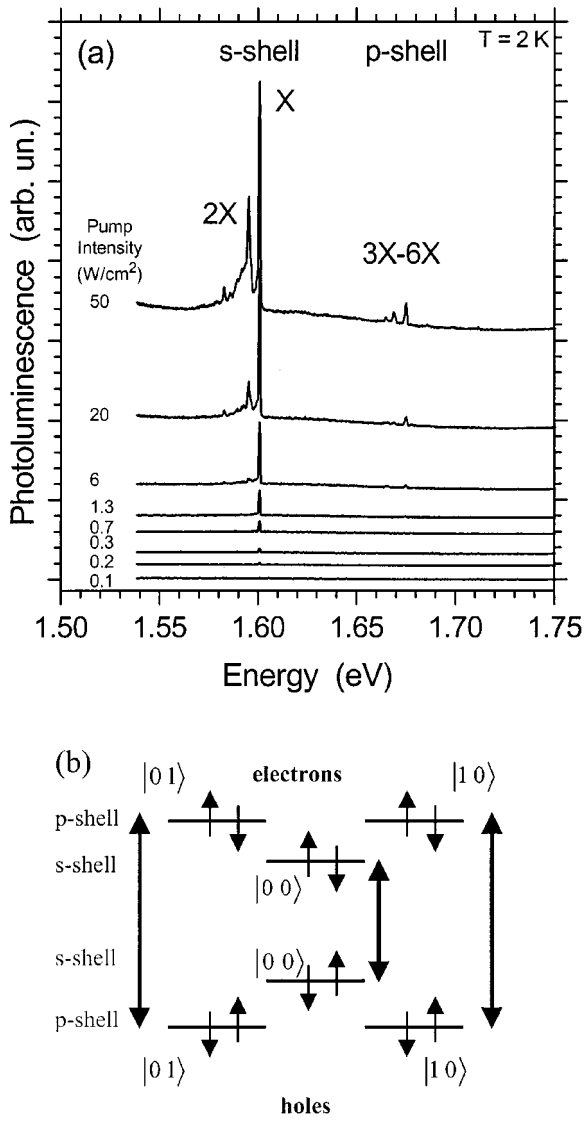

FIG. 3. (a) Photoluminescence spectra of a single $Al_{0.36}In_{0.64}As$ QD for different excitation powers. (b) The two lowest shell configurations for a QD filled with six excitons. The states are denoted $|m\ n\rangle$ and the allowed radiative transitions are shown with arrows.

ton state. The group of lines around the biexciton line is assigned to the recombination of charged excitons. The energy shift of the biexciton line relative to the exciton line arises from the exciton-exciton Coulomb interaction in the QD and can be considered as the biexciton binding energy, the difference between the energies of two uncorrelated excitons and the energy of the two-exciton complex. This value for the biexciton binding energy is larger by ~2 meV compared with values observed in InAs/GaAs QDs.[23,25–26] The appearance and growth of the biexciton line is followed by some filling of the second shell, located at an energy ~70 meV higher than the lowest shell. The two peaks observed in the second shell are associated to recombination of the three-exciton ($3X$) up to the six-exciton ($6X$) complexes. This is supported by the appearance of additional lines in the *s* shell region that are attributed to multicarrier interactions arising from the addition of the third to sixth exciton in the QD.[26,30]

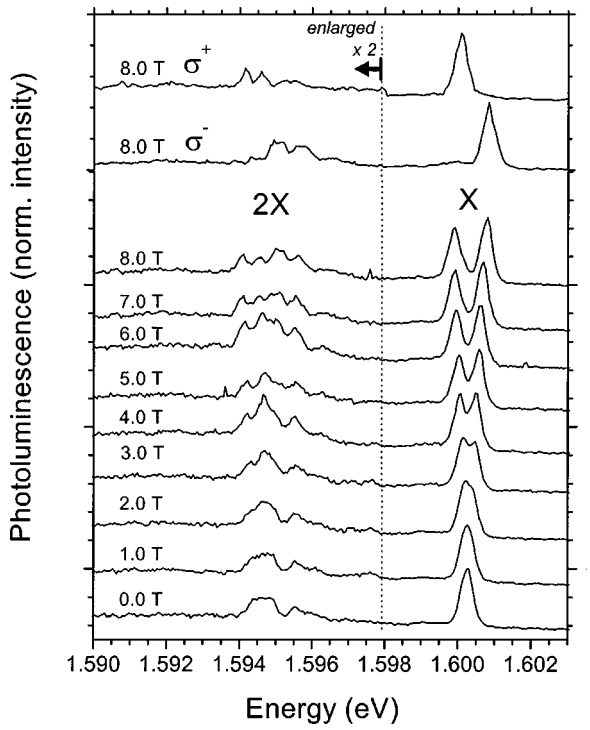

FIG. 4. Single QD photoluminescence spectra recorded at different magnetic fields. Top two curves are polarized photoluminescence spectra recorded at $B = 8.0$ T.

The exciton and biexciton line observed at lower pumping powers are still present in the spectra since statistically at these pump powers, the probabilities of having only one or two electron hole pairs is still high.[33] These two peaks could also be due to the recombination of excited states of the exciton and/or biexciton, where only one exciton at a time is promoted to the second shell,[23,30] although this would not explain the appearance of additional peaks in the lowest shell at higher pump powers.

We are only able to weakly populate the first excited states. However, since the emission from the wetting layer occurs at 1.89 eV and emission from the lowest QD level is at 1.60 eV, we can expect the QD to have approximately four or five groups of bound states (e.g.: 1.60, 1.67, 1.74, 1.81, and 1.88 eV assuming equal spacing of levels). This number of excited states is similar to the one observed in $In_xGa_{1-x}As$ quantum dots.

III. SINGLE QD MAGNETO-PHOTOLUMINESCENCE

Figure 4 shows the photoluminescence spectra of a single QD at different magnetic fields. The excitation power was increased to a level where some biexciton contribution appears in the spectra. The exciton recombination at $B = 0$ T is located at 1.6002 eV. In addition, further emission lines are observed ~5 meV below the exciton, which will be discussed later. In order to facilitate the discussion of these lines they have been enlarged by a factor of two.

Let us first address the behavior of the exciton: as the magnetic field is increased, the exciton emission splits into σ^- polarized at higher energies, and σ^+ polarized at lower

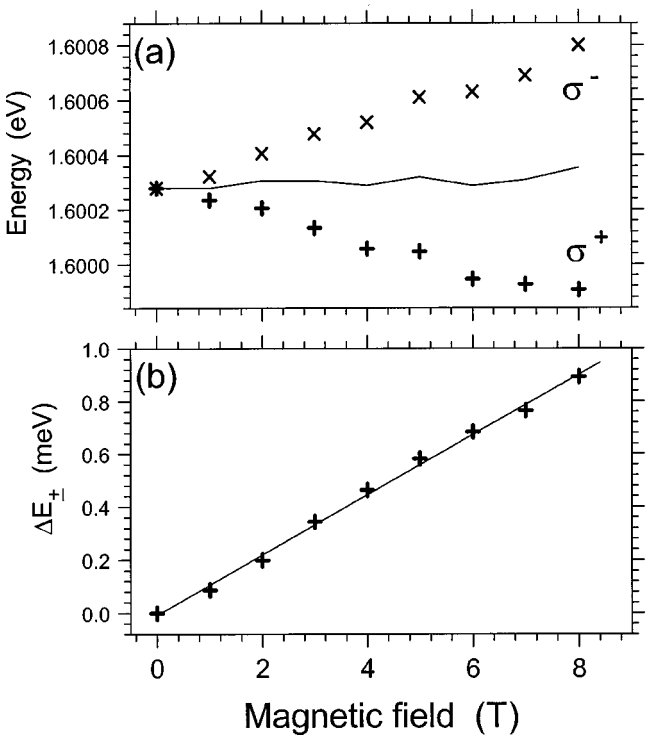

FIG. 5. (a) Exciton energies as a function of the magnetic field. The transitions are labeled corresponding to their different circular polarizations. The solid line corresponds to the center of the exciton doublet. (b) Zeeman splitting of the exciton versus magnetic field.

energies (see the polarization resolved spectra at the top of Fig. 4). This is due to the Zeeman splitting of the exciton, $\Delta E_{\pm} = g_X \mu_B B$, where g_X is the exciton g factor and μ_B is the Bohr magneton. In Fig. 5(a), the energies of the spin-polarized exciton emission line are plotted versus magnetic field. Within the experimental accuracy, the spin splitting between the two emission lines increases linearly with B, as shown in Fig. 5(b). At $B = 8.0$ T, the splitting is as large as 0.9 meV. From the linear regression in Fig. 5(b), we obtain an excitonic g factor $g_X = 1.97 \pm 0.04$. A number of single QDs were studied in this way, and the spin splitting changed only slightly from dot to dot by about ± 0.1 meV. Such small variations are indicative of a high quality material.

Additional information about the exciton can be obtained by looking at the magnetic-field dependence of the center of the exciton doublet in Fig. 5(a), where we observe only a slight diamagnetic shift to higher energies with increasing magnetic field. The shift is less than 0.1 meV in the range of 0 to 8 T, resulting in a diamagnetic coefficient of $0.8 \pm 0.3\,\mu\text{eV/T}^2$. This value is smaller than the $2.6 \pm 0.4\,\mu\text{eV/T}^2$ measured in an earlier study on $In_{0.55}Al_{0.45}As/Al_{0.35}Ga_{0.65}As$ QDs, although in that case, the shift was measured on a large QD ensemble.[34]

Now let us turn to the discussion of the low-energy lines in the spectra in Fig. 4. As indicated above, at $B = 0$ T, the emission consists of two prominent lines, one rather broad emission band located at ~ 1.5945 eV and one at slightly higher energies ~ 1.5956 eV. The latter one shows no dependence on magnetic field (neither a diamagnetic shift nor a spin splitting). Furthermore, it does not show a superlinear dependence on excitation power as does the other feature. Therefore, it is unlikely that it originates from the recombination of excitonic complexes in the QD. It might be related to defect recombination, however, its origin is not clear yet.

The low-energy band shows some structure indicating that it might consist of several emission lines, as is also suggested by its large linewidth as compared to the exciton recombination. However, the small energy separation between them prevents the spectral resolution of several features. Information on the number of spectral lines at $B = 0$ T can be obtained from the magnetic field studies due to spin splitting. In high fields, four prominent lines are observed. Their magnetic-field dependencies are quite similar to that of the exciton. The polarization analysis shows that the two lines at lower energies are σ^+ polarized, while the lines at higher energies are σ^- polarized. From the magnetic dependence we can trace back that the energies of the two low-energy lines of opposite polarization converge for $B \rightarrow 0$ as do the energies of the high-energy doublet. From this observation we conclude that the zero-field emission is mainly a superposition of two spectral lines (the indications for weak additional emission features will be discussed).

However, only one of the two main $B = 0$ T emission lines can be a recombination from the biexciton. It should be noted that the biexciton is a spin singlet state, and thus, its energy cannot be split by a magnetic field. However, the final state of the biexciton transition is an exciton,[35] therefore, the spin splitting of the biexciton emission is given by the Zeeman splitting of the exciton. Therefore, the splitting of the biexciton is identical to that of the exciton.

The other feature could be associated with emission from a singly charged exciton that would also split in the same way as the exciton peak as a function of the magnetic field, because the splitting is given by the g factors of the recombining electron-hole pair. Since the charged exciton can have negative and positive charge (X^- or X^+), in general, six emission lines can be expected in the spectra, while from the experiment, we obtain evidence for four lines only. This might be due to two reasons: (a) First, the creation of one of the charged excitons might be suppressed. To mention only one mechanism for suppression, in the case of X^-, for example, one could imagine that an electron of a trapped exciton tunnels through the $Al_xGa_{x-1}As$ barrier that surrounds the QD towards a defect state at the lateral sidewalls of the field leaving behind a hole in the dot. Together with an additional exciton, this hole will form the X^+ complex. (b) The energy of one of these complexes might be degenerate with the energy of the biexciton.

We note that there are also indications for other emission lines in the spectra that are, however, of rather weak intensity. The appearance of additional spectra becomes possible if the rotational symmetry of the quantum dot system is broken.[36] In this case, angular momentum is no longer a good quantum number and a mixing of bright and dark excitons can occur resulting in an observation of the dark states. Indeed one notes, for example, that the σ^+ polarized component of the exciton shows some high-energy shoulder, which might arise from the recombination of a predomi-

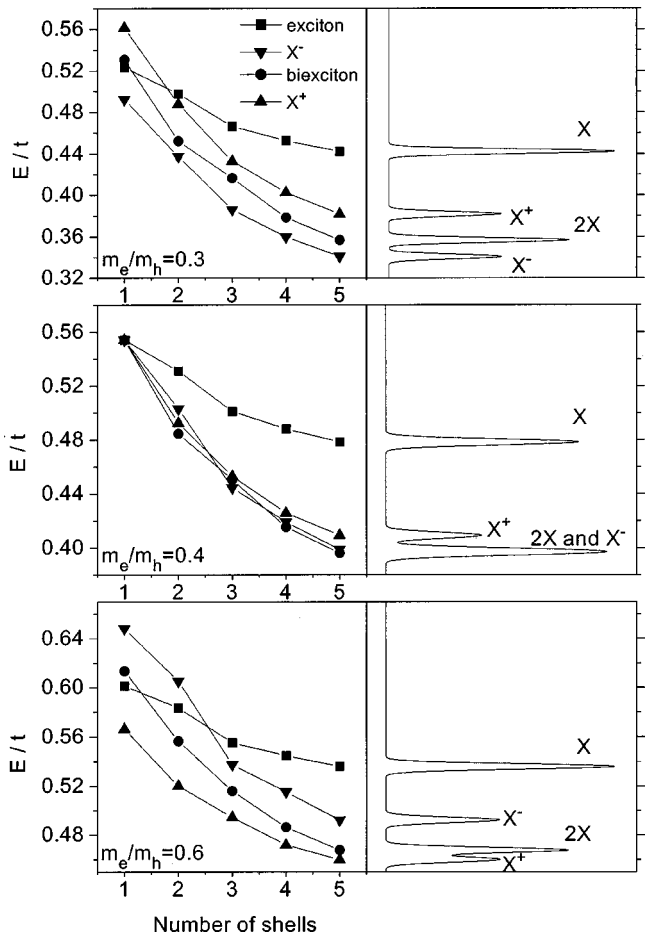

FIG. 6. Calculated exciton, biexciton, and negatively and positively charged exciton emission energies as a function of the number of confined shells for three different ratios of the electron to hole mass. The right-hand side shows the possible emission spectrum for five shells with the arbitrary assigned oscillator strength of each transition. The actual intensities depend on the average population of each species.

nantly dark state. These dark states would naturally also show up in the recombination of the bi- or the charged-exciton complexes, because a predominantly dark electron-hole pair can decay due to the symmetry breaking.

This assignment is supported by calculations of the emission spectrum from the exciton, biexciton, and a negatively and positively charged exciton in a QD using the Hamiltonian of interacting electrons and holes of Ref. 30. We assume an energy level spacing of 50 meV for the electrons and 20 meV for the holes that gives the level spacing of $t = 70\,\mathrm{meV}$. The level spacing t is an important input parameter that circumvents our lack of knowledge of the microscopic parameters of the QD. The ratio of electron-to-hole level spacing is unknown but consistent with simultaneous capacitance and photoluminescence measurements on InAs QDs by Schmidt, Medeiros-Ribeiro, and Petroff in Ref. 37. The remaining parameters are the ratio of the electron to hole mass and the number of confined shells. Figure 6 shows the emission energies from an exciton, biexciton, and a negatively and positively charged exciton as a function of the number of shells for three different ratios of the electron-to-hole mass. We see that the emission energies depend both on the number of shells and on the ratio of masses. The position of the emission line is strongly renormalized by Coulomb interaction. For a single shell, this renormalization accounts for ~50% of total kinetic energy quantization. The renormalization depends further on the type of complex through the number of single-particle levels. This is because different complexes are built from a different number of configurations. For five shells, the number of exciton configurations is $N_X = 29$, biexciton configurations $N_{2X} = 1276$, and charged exciton X^- is $N_{X_-} = 186$. The differences in the energy of the biexciton and charged exciton recombination line appears to be $< 0.02t$. The ratio of electron and hole effective masses $m_e/m_h = 0.4$ is special in that the electron-electron, hole-hole, and electron-hole interactions are almost identical (symmetrical interactions). In this case, the exciton is a neutral complex, a picture consistent with the presence of almost degenerate levels associated with the recombination from the p shell. Assuming therefore $m_e/m_h = 0.4$, the exciton binding energy $\Delta E_{2X} = E_{2X} - 2E_X$ is found to be 5.1 meV, which agrees with the measured value. Similarly, the charged exciton (X^-) emission energy is given by $\Delta E_{X_-} = E_{X_-} - E_X - T_e$ where $T_e = 50\,\mathrm{meV}$ is the single-particle kinetic energy of the electron. The calculated charged exciton binding energy is 4.8 meV, which could correspond to the weak additional peak observed in the spectra. To summarize, the measured emission spectra are consistent with the calculated emission from the exciton, biexciton, and charged exciton complexes.

IV. CONCLUSION

We investigated a single self-assembled $Al_{0.36}In_{0.64}As/Al_{0.33}Ga_{0.67}As$ QD by magneto-photoluminescence spectroscopy and demonstrated the existence of quantized energy levels in these ternary QDs. By varying the excitation power, we measured the recombination spectrum of neutral and charged excitons populating ground and excited states of a quantum dot. We deduced an intersublevel electron and hole energy spacing of ~70 meV, which points to the existence of up to five confined shells in these QDs. The binding energy of a biexciton and charged exciton was found to be ~5 meV. In the magnetic field, we observed a similar Zeeman splitting of the exciton and the biexciton transitions.

ACKNOWLEDGMENTS

Part of this work has been carried out under the Canadian European Research Initiative on Nanostructures supported by the IMS, NRC, NSERC, and EC. K.H. thanks the NSERC for financial support, and P. H. thanks the Alexander von Humboldt Foundation for partial support. The Würzburg Group gratefully acknowledges the financial support by the State of Bavaria and by the Deutsche Forschungsgemeinschaft.

[1] For an overview, see L. Jacak, P. Hawrylak, and A. Wojs, *Quantum Dots* (Springer-Verlag, Berlin, 1998).
[2] *Self-Assembled* $In_xGa_{1-x}As/GaAs$ *Quantum Dots*, edited by M. Sugawara (Academic, San Diego, 1999).
[3] S. Fafard, H. C. Liu, Z. R. Wasilewski, J. McCaffrey, M. Spanner, S. Raymond, C. Nì. Allen, K. Hinzer, J. Lapointe, C. Struby, M. Gao, P. Hawrylak, C. Gould, A. Sachrajda, and P. Zawadzki, Proc. SPIE **4078**, 100 (2000).
[4] S. Fafard, J. L. Merz, D. Leonard, and P. M. Petroff, in *Nanostructures and Quantum Effects*, edited by H. Sakaki and H. Noge (Springer-Verlag, Berlin, 1994), p. 225.
[5] S. Fafard, K. Hinzer, S. Raymond, M. Dion, J. McCaffrey, Y. Feng, and S. Charbonneau, Science **274**, 1350 (1996).
[6] S. Fafard, Z. R. Wasilewski, C. Ni. Allen, D. Picard, M. Spanner, J. P. McCaffrey, and P. G. Piva, Phys. Rev. B **59**, 15 368 (1999).
[7] S. Fafard, R. Leon, D. Leonard, J. L. Merz, and P. M. Petroff, Phys. Rev. B **52**, 5752 (1995).
[8] K. Mukai, N. Ohtsuka, H. Shoji, and M. Sugawara, Appl. Phys. Lett. **68**, 3013 (1996).
[9] R. Leon, S. Fafard, P. G. Piva, S. Ruminov, and Z. Lilietal-Weber, Phys. Rev. B **58**, R4262 (1998).
[10] G. Park, O. B. Shchekin, D. L. Huffaker, and D. G. Deppe, Appl. Phys. Lett. **73**, 3351 (1998).
[11] Y. Sugiyama, Y. Nakata, T. Futatsugi, M. Sugawara, Y. Awano, and N. Yokoyama, Jpn. J. Appl. Phys., Part 2 **36**, L158 (1997).
[12] M. Grundmann, N. N. Ledentsov, O. Stier, D. Bimberg, V. M. Ustinov, P. S. Kop'ev, and Zh. I. Alferov, Appl. Phys. Lett. **68**, 979 (1996).
[13] H. Lipsanen, M. Sopanen, and J. Ahopelto, Phys. Rev. B **51**, 13 868 (1995).
[14] S. Fafard, R. Leon, D. Leonard, J. L. Merz, and P. M. Petroff, Phys. Rev. B **50**, 8086 (1994).
[15] R. Leon, S. Fafard, D. Leonard, J. L. Merz, and P. M. Petroff, Appl. Phys. Lett. **67**, 521 (1995).
[16] S. Raymond, S. Fafard, S. Charbonneau, R. Leon, D. Leonard, P. M. Petroff, and J. L. Merz, Phys. Rev. B **52**, 17 238 (1995).
[17] K. Hinzer, A. J. SpringThorpe, E. M. Griswold, J. Lapointe, Y. Feng, A. Delâge, and S. Fafard, J. Appl. Phys. **87**, 1496 (2000).
[18] J.-Y. Marzin, J. M. Gerard, A. Israel, D. Barrier, and G. Bastard, Phys. Rev. Lett. **73**, 716 (1994).
[19] R. Leon, P. M. Petroff, D. Leonard, and S. Fafard, Science **267**, 1966 (1995).
[20] A. Zrenner, L. V. Butov, M. Hagn, G. Abstreiter, G. Böhm, and G. Weimann, Phys. Rev. Lett. **72**, 3382 (1994).
[21] M. Grundmann, J. Christen, N. N. Ledentsov, J. Böhrer, D. Bimberg, S. S. Ruvimov, P. Werner, U. Richter, U. Gösele, J. Heydenreich, V. M. Ustinov, A. Yu. Egorov, A. E. Zhukov, P. S. Kop'ev, and Zh. I. Alferov, Phys. Rev. Lett. **74**, 4043 (1995).
[22] D. Gammon, E. S. Snow, and D. S. Katzer, Appl. Phys. Lett. **67**, 2391 (1995).
[23] A. Kuther, M. Bayer, A. Forchel, A. Gorbunov, V. B. Timoteev, F. Schäfer, and J. P. Reithmaier, Phys. Rev. B **58**, R7508 (1998).
[24] E. Dekel, D. Gershoni, E. Ehrenfreund, D. Spektor, J. M. Garcia, and P. M. Petroff, Phys. Rev. Lett. **80**, 4991 (1998).
[25] F. Findeis, A. Zrenner, G. Böhm, and G. Abstreiter, Solid State Commun. **114**, 227 (2000).
[26] M. Bayer, O. Stern, P. Hawrylak, S. Fafard, and A. Forchel, Nature (London) **405**, 923 (2000).
[27] L. Landin, M.-E. Pistol, C. Pryor, M. Persson, L. Samuelson, and M. Miller, Phys. Rev. B **60**, 16 640 (1999).
[28] Y. Toda, T. Sugimoto, M. Nishioka, and Y. Arakawa, Appl. Phys. Lett. **76**, 3887 (2000).
[29] Z. R. Wasilewski, S. Fafard, and J. P. McCaffrey, J. Cryst. Growth **201**, 1131 (1999).
[30] P. Hawrylak, Phys. Rev. B **60**, 5597 (1999); A. Wojs and P. Hawrylak, Solid State Commun. **100**, 2487 (1996).
[31] O. Stier, M. Grundmann, and D. Bimberg, Phys. Rev. B **59**, 5688 (1999).
[32] H. Jiang and J. Singh, Appl. Phys. Lett. **71**, 3239 (1997); L. W. Wang, A. J. Williamson, A. Zunger, H. Jiang, and J. Singh, *ibid.* **76**, 339 (2000).
[33] S. Raymond, X. Guo, J. L. Merz, and S. Fafard, Phys. Rev. B **59**, 7624 (1999).
[34] P. D. Wang, J. L. Merz, S. Fafard, R. Leon, D. Leonard, G. Medeiros-Ribeiro, M. Oestreich, P. M. Petroff, K. Uchida, N. Miura, H. Akiyama, and H. Sakaki, Phys. Rev. B **53**, 16 458 (1996).
[35] M. Bayer, T. Gutbrod, A. Forchel, V. D. Kulakovskii, A. Garbunov, M. Michel, R. Steffen, and K. H. Wang, Phys. Rev. B **58**, 4740 (1998).
[36] M. Bayer, A. Kuther, A. Forchel, A. A. Gorbunov, V. B. Timofeev, F. Schafer, J. P. Reithmaier, T. L. Reinecke, and S. N. Walck, Phys. Rev. Lett. **82**, 1748 (1999).
[37] K. H. Schmidt, G. Medeiros-Ribeiro, and P. M. Petroff, Phys. Rev. B **58**, 3597 (1998).